National Aeronautics and
Space Administration

Artemis Campaign Development
ACD-50044
INITIAL RELEASE

EFFECTIVE DATE: OCTOBER 6, 2022

LUNAR SURFACE DATA BOOK

REVISION AND HISTORY PAGE

Revision No.	Change No.	Description	Effective Date
-	ACD-C0032	Initial Baseline Release (Reference Artemis Campaign Development (ACD) Control Board (ACB), dated 10/06/22)	10/06/22

TABLE OF CONTENTS

SECTION **PAGE**

1.0 INTRODUCTION

1.1 PURPOSE

Artemis missions will need to reference and work with a common set of lunar surface data, products, and analytical assumptions to accomplish Artemis mission science, exploration, and operational objectives. This Lunar Surface Data Book is intended to be used as a reference for candidate vendors and agency personnel who are addressing Artemis lunar surface challenges to ensure a common set of data sources and assumptions when interpreting remote sensing data specific to the needs of surface mission planning.

1.2 SCOPE

This document provides a common reference set of existing lunar surface data, products, analytical assumptions, and representative use cases to be incorporated into Artemis surface mission planning efforts. This document pertains solely to the surface of the Moon and the ecosystem of data and products to be used to describe the lunar surface.

1.3 CHANGE AUTHORITY/RESPONSIBILITY

NASA Office of Primary Responsibility (OPR) identified for this document is ACD Systems Engineering & Integration (SE&I). Proposed changes to this document shall be submitted via a Change Request (CR) to the appropriate ACD Control Board for consideration and disposition. All such requests shall adhere to the ACD Configuration Management Process documented in ACD-50005, ACD Configuration and Data Management Plan.

2.0 DOCUMENTS

2.1 APPLICABLE DOCUMENTS

The following documents include specifications, models, standards, guidelines, handbooks, and other special publications. The documents listed in this paragraph are applicable to the extent specified herein.

Document Number	Document Title
HEOMD-410 V1	HEO Lunar Traverse Data Book
VIPER-ROV-SE-SPEC-002	VIPER Rover Obstacle Definition
SLS-SPEC-159	Cross Program Design Specification for Natural Environments (DSNE)

2.2 REFERENCE DOCUMENTS

The following documents contain supplemental information to guide the user in the application of this document. Additional references to data sources in this document can be found in Appendix B.

Document Number	Document Title

3.0 LUNAR SURFACE DATA SOURCES

HEOMD-003 lists SLS-SPEC-159 Design Specifications for Natural Environments (DSNE) as the baseline source for all lunar environments. Per HEOMD-003, DSNE is a mandatory engineering technical authority document and is fully applicable.

Between 1963 and 1972, the Moon was a focus of an intense, integrated program of American exploration including robotic orbiters (Lunar Orbiter) and impactors (Ranger), soft landers (Surveyor) and crewed missions (Apollo). In the 21st Century, an ambitious flotilla of international missions has developed a modern view of the Moon and its surface. These modern missions (e.g., the JAXA Kaguya, ESA Smart 1, NASA/DOD Clementine, NASA Lunar Prospector, ISRO Chandrayaan-1, NASA GRAIL, NASA LADEE, NASA LCROSS, and NASA Lunar Reconnaissance Orbiter) have all dramatically increased our understanding of the Moon's environment. Therefore, the Moon is the one planetary object besides Earth that has been systematically studied for over five decades from a variety of perspectives including remote observations, in situ measurements, human field work, and returned samples with appropriate geological context. With that full suite of data sources, lunar scientists and mission planners today have access to several data sources and products that characterize the lunar surface, making the Moon the most well-understood and well-characterized body in our solar system besides Earth. That relative wealth of knowledge compared to other solar system objects, especially when compared to the spartan state of our knowledge prior to the Apollo missions, enables 21st century lunar mission planners to optimize systems, do detailed mission planning, and enable transformative lunar science and exploration outcomes with future missions. This section describes the sources of data before reviewing the data themselves and only the most recent and relevant data is included.

This document deals entirely with data that presently exists and is readily available in NASA's Planetary Data System with detailed explanations and interpretation available in peer-reviewed literature. Future SMD Lunar Discovery and Exploration Program missions to the lunar poles will improve our understanding of lunar surface characteristics, but those missions have not yet occurred and presently play no role in mission planning. The emphasis in this document is placed on the data from US missions, particularly that from the Lunar Reconnaissance Orbiter, because the provenance of those data is well-understand and fully characterized, and all LRO source data is fully and publicly available per long-standing NASA Policy.

3.1 IN SITU LUNAR SURFACE DATA

A robust set of surface data exists for the multiple landing sites visited by NASA missions (Surveyor and Apollo). Data for surface (regolith) geotechnical and rock abundance properties is derived from both images/observations and physical measurements of the surface. The Lunar Sourcebook includes geotechnical data from the U.S.S.R. Lunokhod 1 and 2 uncrewed rovers that traversed 47 km of the lunar surface and collected ~1000 cone vane penetrometer measurements of the upper 10 centimeters of the regolith (Heiken et al., 1991). Much of the data from the 1960-1970s is not in modern formatting, rather preserved as film negatives or tabular data formats. That said, the in-situ data presents our best understanding of the specific properties of the lunar surface which are directly applicable to Artemis mission planning. Given that, care must be used to not over-interpret landing site data that is *not* relevant to the lunar south pole. For example, much consternation could rise from assuming any site is similar to the rocky surface encountered by the Surveyor VII mission, which landed (autonomously) and without any active hazard avoidance in the rockiest region yet explored on the Moon. We have no reason to believe the south pole region will be in any way similar to that particular landing site. Instead, Artemis landing sites will be in the lunar highlands of the south pole region, resulting in operations much more comparable to the Apollo 14 and 16 landing sites. Data from these missions are available through NASA's Planetary Data System (PDS), NASA's Space Science Data Coordinated Archive (NSSDC), and the PDS' Analyst Notebook.

3.2 ORBITAL DATA RELEVANT TO THE SURFACE

NASA has sent numerous missions to lunar orbit to understand the lunar surface and its environment, leading to the largest volume of data for any planetary body outside of the Earth. This document focuses on the data that is directly related to the lunar surface and the properties that are derived from them. The most recent and directly relevant source of data on the lunar surface is from the Lunar Reconnaissance Orbiter (LRO), sent to the Moon with the explicit goal of developing the data needed to support landing site selection and validation. , Since 2010, LRO's has been in a stable frozen orbit with periapsis centered on the South Pole, enabling a significantly longer mission duration and a substantial amount of data is now available for the south polar region, giving us the best possible dataset to identify the scientifically interesting, and relatively safe, sites to explore.

3.2.1 Lunar Reconnaissance Orbiter Data

The Lunar Reconnaissance Orbiter (LRO) was launched on 18 June 2009 from what is now Cape Canaveral Space Force Station and remains in lunar orbit and operational as of May 2022 with funded operations until at least October 2025, spacecraft health non-withstanding. LRO was designed to meet the requirements of the former Exploration Systems Mission Directorate (ESMD) to identify safe landing sites for human and robotic missions to the Moon, understand the lunar radiation environment, and characterize potential lunar resources. LRO spent several months in an elliptical, stable frozen 30 x 216 km orbit with apoapsis over the lunar South Pole, then transitioned for the next two years into a 50x50 km circular polar mapping orbit. Following the completion of its baseline mapping mission, LRO then transitioned again into a quasi-stable 30 x 216 km polar orbit which has slowly evolved to a nearly circular 100 km orbit, where it remains today. Despite the natural procession of the orbit away from direct south polar overflights, it is still possible that additional LROC images can be targeted for select areas in the polar regions; please contact the LRO Project Scientist, Dr. Noah Petro, for additional information. The LRO mission instrument suite and scientific outcomes have been well-described in multiple publications, including Vondrak et al. 2010 and Keller et al. 2017. Briefly, LRO carries seven instruments, each designed to investigate a specific aspect of the lunar environment relevant to future exploration. We briefly summarize the LRO instrument suite in this section.

3.2.1.1 The Cosmic Ray Telescope for the Effects of Radiation (CRATER)

The primary goal of CRaTER is to characterize the lunar radiation environment in terms of the different types of charged particles and their energies, particularly above 10 MeV, to better understand what hazards future human explorers will be subjected to. Radiation comes from the Sun and beyond the Solar System (galactic cosmic rays). These data have allowed scientists to determine the potential biological impacts of the radiation. CRaTER also tests models of radiation effects and shielding and measure radiation absorption by human tissue-like plastic, aiding in the development of protective technologies to help keep crews safe.

3.2.1.2 Diviner Lunar Radiometer Experiment (DLRE)

The objective of DLRE (more commonly referred to as Diviner) is to measure lunar surface temperatures at scales that provide essential information for future surface operations and exploration. The temperature of the lunar surface and subsurface is a critical environmental parameter for future human and robotic exploration. While the Apollo missions were all targeted to equatorial landing sites and were only conducted during the lunar day, NASA's new lunar exploration program will involve exploration of much higher latitudes eventually involving astronaut stays of longer than two weeks. A key Diviner objective is to determine the temperatures within permanently shadowed areas, to understand the potential of these areas to harbor water ice. Orbital thermal mapping measurements also provide detailed information on surface parameters such as composition, hazards, rough terrain, or rocks. The Diviner instrument is able to determine surface temperatures to within 5 °C across areas as small as 300 m using 9 different wavelengths between 7 and 200 microns.

Diviner seasonal bolometric temperature data products are commonly used for preliminary evaluation of polar regions of interest. These include the Maximum, Average, Minimum and Amplitude rasters at 240 meters per pixel (Williams et al., 2019). The data product descriptions and links to seasonal and hourly temperature products are available from the project team's website.

Data | diviner (ucla.edu)

Index of /~jpierre/diviner/level4_polar/additional_maps (ucla.edu)

The seasonal temperature grids are available from NASA's Moon Trek by searching for the Temperature product type.

Moon Trek (nasa.gov)

The Diviner data is available from the PDS archive at different levels of processing.

PDS Geosciences Node Data and Services: LRO DIVINER (wustl.edu)

3.2.1.3 Lyman Alpha Mapping Project (LAMP)

LAMP is an imaging ultraviolet spectrometer, detecting UV light between 1200-1800 Å with an effective surface spatial resolution of up to 200 m per pixel near the poles (Gladstone et al. 2010). The goal of LAMP is to map the entire lunar surface in the far ultraviolet part of the spectrum, including areas in Permanent Shadow. LAMP searches for surface ice and frost in the polar regions, providing images of permanently shadowed regions illuminated only by starlight and the glow of interplanetary hydrogen emission, known as the Lyman Alpha line.

3.2.1.4 Lunar Exploration Neutron Detector (LEND)

LEND is a neutron spectrometer similar to another instrument, the High Energy Neutron Detector (HEND) on the Mars Odyssey spacecraft. LEND indicates the distribution of surface and subsurface hydrogen through interpretations of detections of the epithermal neutron flux (0.4 eV-100 eV) at various spatial resolutions depending on orbital altitude. Due to LRO's polar orbit configuration, LEND data is densest, and therefore of highest resolution, in areas around the south pole.

3.2.1.5 Mini-RF

Mini-RF (Raney et al. 2010) was an advanced synthetic aperture radar, capable of measurements in X-band and S-Band, designed to provide observations of the permanently shadowed areas on the Moon using radar illumination at resolutions of 30 and 150 meters. The intent of the Mini-RF experiment was to determine whether ice was present in significant quantities in the lunar polar regions, as well as to map rock distributions on the lunar surface and subsurface. The instrument no longer has the capability to transmit radar signals, only to receive them. Therefore, it now operates in a receive-only mode measuring bistatic radar signals transmitted from ground-based radio telescopes and reflected off the lunar surface.

3.2.1.6 Lunar Orbital Laser Altimeter (LOLA)

The LOLA instrument (Smith et al. 2010) pulses a single laser at 1064 nm wavelength, splitting the output into five separate beams that illuminates the lunar surface 28 times per second. For each beam, LOLA measures the time of flight (range), pulse spreading (surface roughness), and transmit/return energy (surface reflectance). This allows the topography to be determined, along with an indication of whether the surface is rough or smooth at scales relevant for Exploration planning. LOLA is the "fundamental" dataset for all LRO instruments, providing the foundational global lunar topographic model and geodetic grid that will serve as the framework to enable precise positioning, safe landing, and surface mobility, as well as characterizing the polar illumination environment.

3.2.1.7 Lunar Reconnaissance Orbiter Camera (LROC)

LROC consists of three cameras (Robinson et al., 2010). There are two Narrow Angle Cameras (NACs) that provide panchromatic images over a 5-km swath from the 50km nominal mapping orbit, with resolutions varying from 0.5-3 m/pixel, depending on orbital altitude. There is also a Wide-Angle Camera (WAC), which provides multispectral images with a pixel scale of 100 m/pixel over seven color bands with a 60-km swath. LROC is designed to address fundamental exploration objectives, including characterizing potential landing sites at the meter scale, mapping regions of permanent shadow or illumination, creating high-resolution maps of the lunar surface, including polar massifs with permanent or near-permanent illumination, observing regions from multiple angles to derive high-resolution meter-scale topography, map the global distribution of the mineral ilmenite, a key lunar resource, create a global morphology base map, characterize lunar regolith, and establish impact hazards.

4.0 LUNAR SURFACE DATA PRODUCTS

4.1 FOUNDATIONAL PRODUCTS

Foundational lunar surface data products are essential descriptive elements built from the raw data collected by instruments described in Section 3. Foundational data products for lunar exploration have recently been described by Laura and Beyer (2021) and the joint LEAG-

MAPSIT Lunar Critical Data Products Specific Action Team (MAPSIT, 2021). Some definitions of key foundational products are briefly summarized here based upon those sources. The intent of this section is to succinctly describe existing data products that are presently being used for mission planning purposes and provide information on relevant descriptive peer-reviewed publications and expedited ways of accessing relevant source data products.

4.2 VISIBLE IMAGERY

While many subclassifications are possible, in general, visible wavelength imagery of the lunar surface (meaning observations produced by sensors designed to collect data in the visible spectrum wavelengths from 380 to 750 nanometers) can be broken down into three categories. The first two categories, Nadir Imagery (described in section 4.2.1.1) and Oblique Imagery (described in section 4.2.1.2), are defined based on the geometry of the camera relative to the surface from orbit. The third category, Image Mosaics (described in section 4.2.1.3), involves executing geodetic and cartographic processing to combine many smaller images into a larger mosaic useful for precision mapping and analyses. Figure 4.2.1 provides an idealized representation of image geometries.

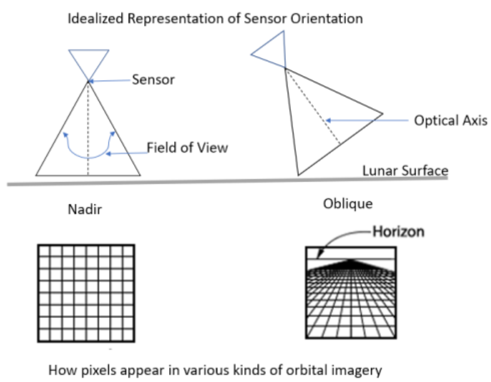

Figure 0.1 Definitions of Sensor Orientation.

4.2.1.1 Nadir Imagery

Nadir imagery is captured from orbit where the camera lens is directly pointing down the nadir direction to the surface. The Narrow Angle Cameras aboard LRO are examples of body-fixed imaging systems whose default mode of operation is a nadir orientation. Figure 4.2.2 is an example of nadir imagery produced by the LROC system.

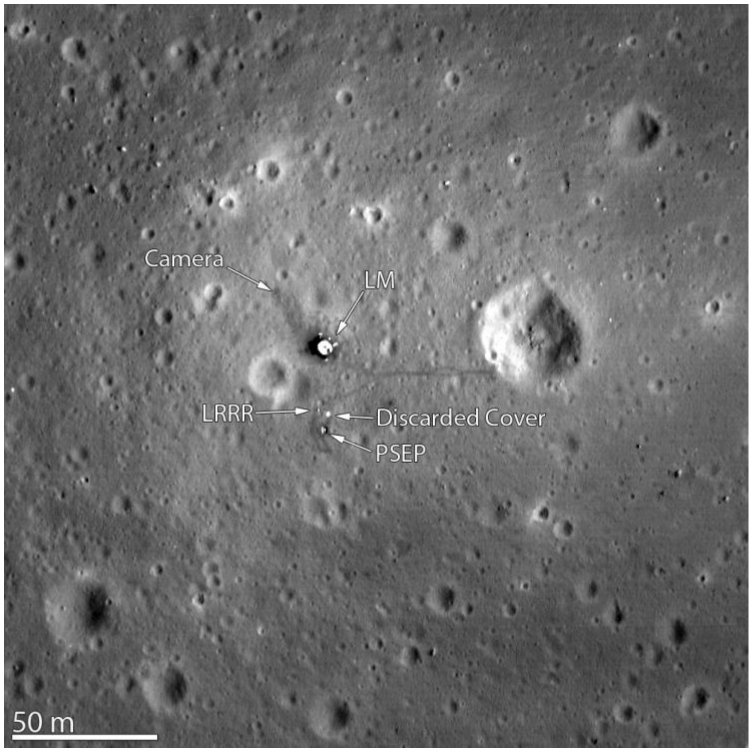

Figure 0.2 Annotated example nadir image of the Apollo 11 landing site and anthropomorphic artifacts at Statio Tranquillitatis, imaged by LRO in 2011. The remnants of Armstrong and Aldrin's historic first steps onto the lunar surface are seen as dark paths

4.2.1.2 Oblique Imagery

Orbital imagery is captured when the orbiting camera lens is canted off the surface normal, resulting in an oblique angle. Although LROC is body-fixed, nadir pointing instrument, with sufficient advance planning, LRO has the capability to roll the spacecraft to obtain oblique images with its Narrow Angle Camera system useful for context interpretation and validating lighting models. An example of an oblique image is provided as figure 4.2.3

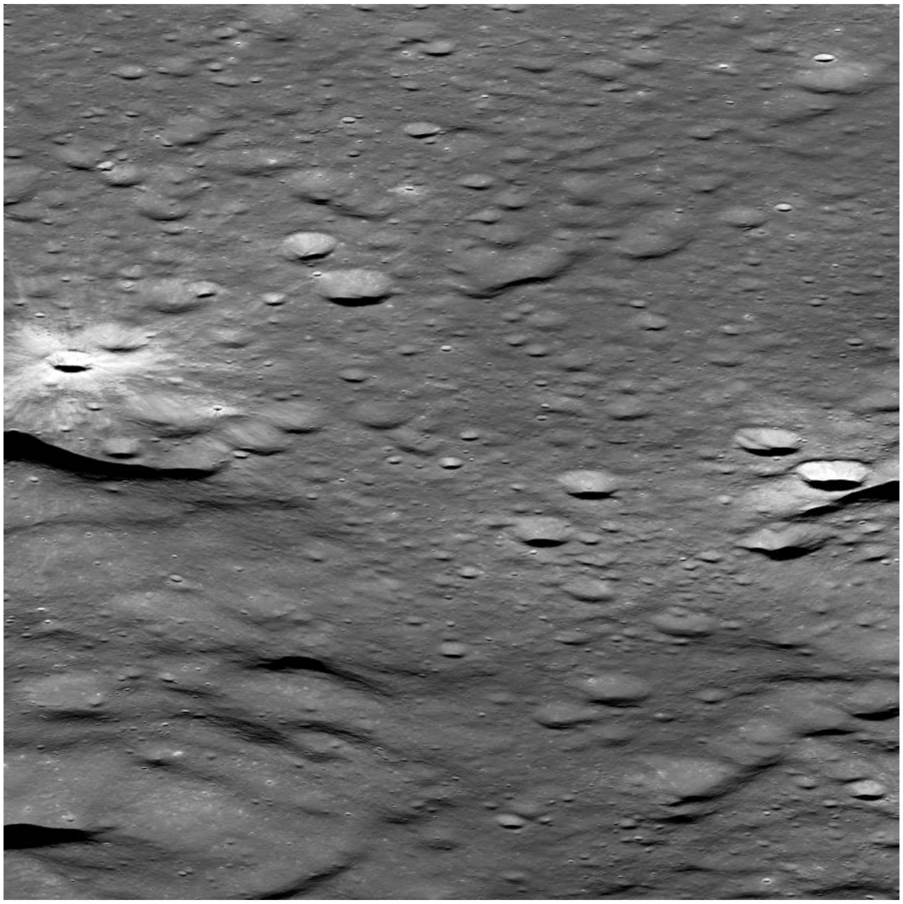

Figure 0.3 Oblique LROC NAC image of the Apollo 16 landing site. Viewpoint is east to west. South Ray crater is center left and North Ray crater is center right. Distance between the two center craters is 10.5 km. Subset of LROC NAC M192817484LR [NASA/GSFC/Arizon]

4.2.1.3 Mosaics

A visible imagery mosaic is an assemblage of overlapping remotely sensed visible wavelength images whose edges have been matched cartographically to create a continuous photographic representation of a portion of the Moon's surface. There are two broad subcategories of image mosaics, uncontrolled and controlled mosaics.

4.2.1.3.1 Uncontrolled Mosaics

An uncontrolled mosaic is a mosaic that comprised of images collected under consistent illumination conditions, and whose edges have been matched from image to image without reference to established geodetic control. Seams between distinct images may or may not be visible. An example of an uncontrolled mosaic is provided as Figure 4.2.4 (notice seams are visible in this Figure). An uncontrolled mosaic of the south polar region has been assembled by the LRO Science Team using LRO NAC images and can be downloaded from the LROC subnode of the PDS Imaging and Cartographic Sciences Node (Viewing South Pole NAC Mosaic (asu.edu))

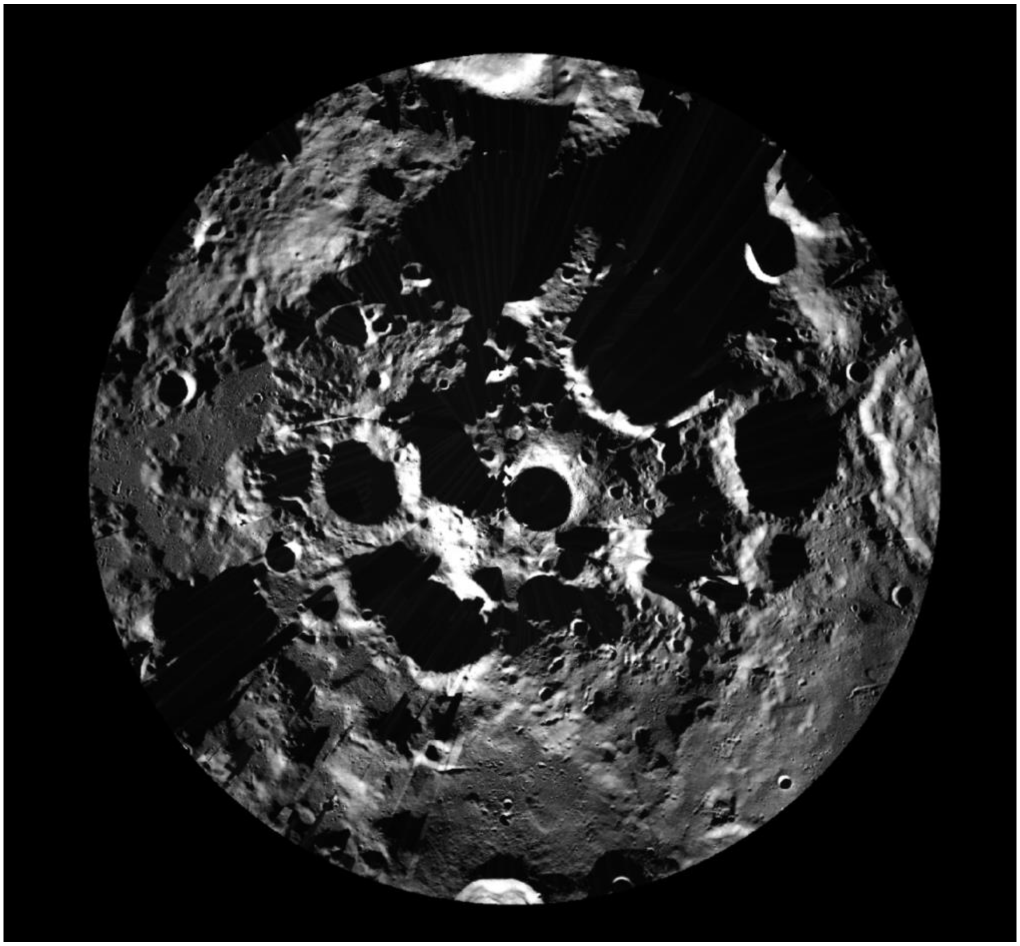

Figure 0.4 Uncontrolled mosaic of 1293 LROC NAC images of the south pole of the Moon, projected in polar stereographic, with a scale of 1 m/pixel from 85.5 - 90 degrees S.

4.2.1.3.2 Controlled Mosaics

Controlled visible imagery mosaics are mosaics comprised of images that have been radiometrically, geometrically, and photometrically corrected to establish an accurate cartographic framework for regional areas of interest (e.g., Martin et al., 2019). Controlled mosaics produced by the LRO team are referred to as Feature Mosaics and are comprised of NAC images created on sequential orbits. The geodetic control process reduces locational uncertainty and ensures accurate distances can be measured from surface features found within the mosaic. An example of a controlled mosaic from a nonpolar region is provided as Figure 4.2.5. Controlled mosaics of LROC WAC frames for the south polar region have been produced by the LROC team (https://wms.lroc.asu.edu/lroc/view_rdr/WAC_ROI_SOUTH_SUMMER) and the US Geological Survey (available online at trek.nasa.gov/moon)

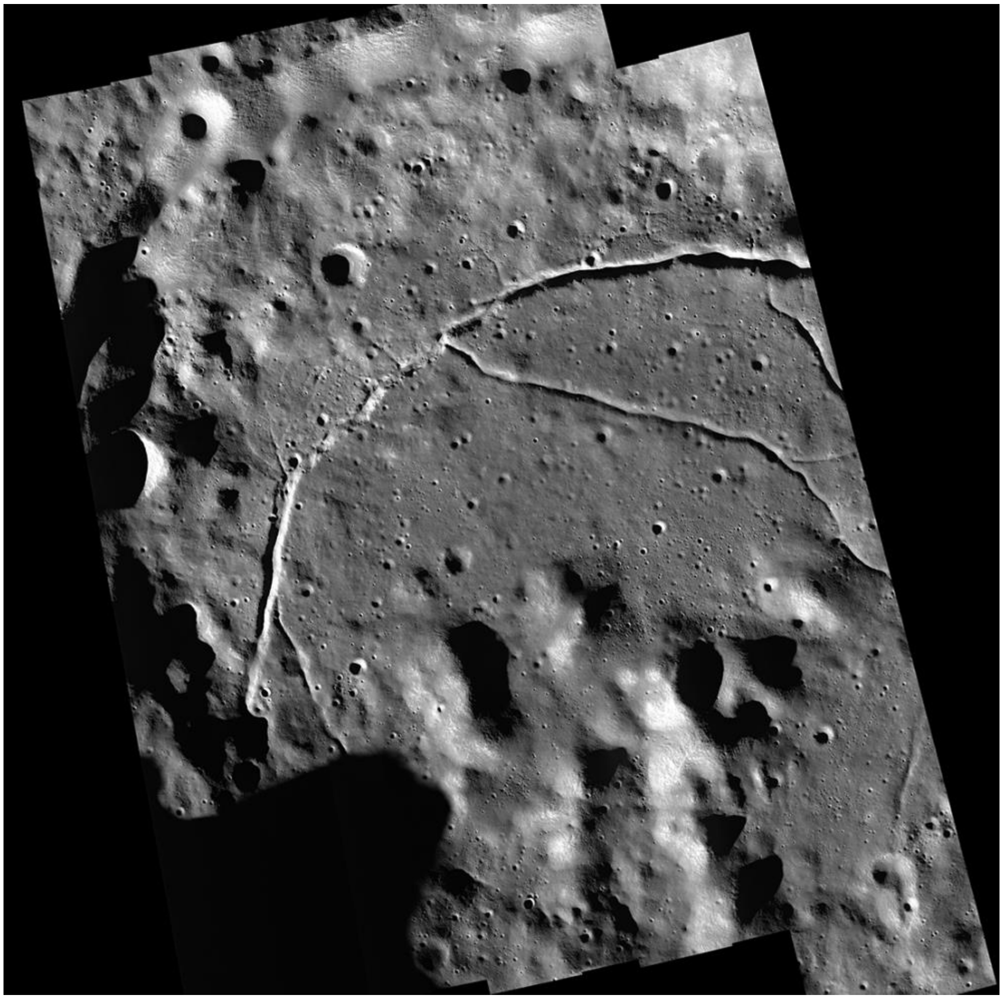

Figure 0.5 A seamless mosaic of a portion of Karpinsky crater (72.61 degrees N, 166.80 degrees East). Scene is 55 km across. NAC images M130949659L/R, M1309503618L/R, M1309510644L/R, M1309517669L/R.

4.2.2 Topographic Data Products

The shape of the lunar surface is described within several complementary topographic data products. Several high-quality topographic products are available for the lunar south pole described below. Topography is one of three primary classes of foundational data products as described in Laura and Beyer (2021).

Generally, there are three categories of terrain models, defined as follows:

- **Digital Elevation Model (DEM):** A digital representation of the topographic surface of a body that excludes natural or built surface objects.

- **Digital Terrain Model (DTM):** A digital representation of the topographic surface of a body that excludes natural or built surface objects but does include natural/built features as vector features.

- **Digital Surface Model (DSM):** A digital representation of the topographic surface of a body, including natural or built surface objects.

Currently, the lunar south pole does not host built surface objects. Preliminary mapping of natural surface objects (boulders, etc.) has begun, but is not yet formalized. For this reason, current topographic products are typically DEMs, although this is expected to change with future surface characterization and activity. Topographic products from several sources are described in the following subsections.

4.2.2.1 South Pole LOLA DEM Mosaic

The shape of the lunar surface is directly measured from orbit by Lunar Orbiter Laser Altimeter (LOLA). Point measurements are then interpolated into gridded data products. Because of the orbit of LRO, LOLA points are densely clustered at high latitudes, enabling gridded topographic maps at 5m/pixel resolution covering much of the South Pole.

This 5m/pixel product represents a significant improvement over previous LOLA releases. By iteratively co-adjusting the LOLA tracks in a self-consistent fashion, orbital errors were reduced by over a factor of 10 such that the new track geolocation uncertainty is ~10 - 20 cm horizontally and ~2 - 4 cm vertically over each region. The new 5 m/pix LDEM is substantially more realistic than previous products with fewer artifacts due to orbital errors and fewer spurious noise points. While the fraction of interpolated 5-m pixels in this polar LDEM is necessarily large (~90%) due to LOLA's cross-track and inter-spot spacing, this LDEM has the advantage of having accurate geodetic control and of being unaffected by shadows, and, thus, will be complementary to higher-resolution topographic models derived solely from imagery.

This product was constructed from 97 individual 20x20 km fields with 2 km overlaps. Each field was processed with the same method as described in Barker et al. (2021). The fields were then individually aligned to the original DEM with a rigid 3-D translation and blended with a cosine taper weight in the overlap regions. The counts (ldec) maps of the individual fields were blended in the same way. Hence, non-integer counts exist in the overlap regions of the final mosaicked product.

The LDEM height and slope uncertainties within the have a stated median RMS Z error ~ 0.30 - 0.50 m (see Barker et al (2021) for a full description of source data and error deviation). Interpolation error depends primarily on gap size, or areal density of the LOLA points, with a secondary dependence on terrain slope that becomes more important over highly sloped terrain. Hence, the interpolation error will be larger at greater distances from the pole for the same pixel scale, because of the lower point density and poorer effective resolution.

Metadata products such as count maps and RMS error maps are available. Interpolation errors are quantifiable and manageable.

The LOLA DEM products are the "foundation" for all LRO data products; all LROC images are controlled to the LOLA dataset.

A mosaic covering all latitudes poleward of 87 deg. S is available here:

PGDA - South Pole LOLA DEM Mosaic (nasa.gov)

Several additional sites of interest are available here:

PGDA - High-Resolution LOLA Topography for Lunar South Pole Sites (nasa.gov)

A full description of data source calibration/corrections and error deviations is available in Barker et al (2021).

Additional LOLA DEM products covering the wider polar regions are available through the Planetary Data System.

4.2.2.2 LROC NAC DTM: Stereo Observations

The two Narrow Angle Cameras (NAC) aboard LRO were not designed as stereo imaging system. However, stereo observations can be acquired over two or more orbits by slewing the spacecraft (Robinson et al., 2010). Globally, a number of these 'stereo pairs" have been collected, comprising approximately 3% of the lunar surface. As described in Henriksen et al. (2017), these pairs are then reduced into Digital Terrain Models at the 2-4 m pixel scale using a consistent set of procedures leveraging the SOCET SET software from BAE systems in combination with the USGS Integrated Software for Imagers and Spectrometers (ISIS) (Anderson et al., 2004, Keszthelyi et al. 2013). By enabling quantitative investigations of elevation, slope, volume, and roughness, complex scientific questions and engineering site suitability assessments can both be comprehensively addressed, rendering NAC DTMs invaluable for both engineering and scientific purposes.

These products offer spatial resolution of up to 2-4 meters/pixel, with vertical accuracy of <1m and horizontal accuracy of <10 m.

As of May 2022, three LROC NAC stereo observations have been have been reduced into publicly-available DTMs and can be downloaded from the LROC subnode of the PDS Imaging and Cartographic Sciences data node:

Terrain Between Nobile and Malapert Craters.

Peak near Spudis crater on the Shackleton-deGerlache connecting ridge.

Malapert Massif.

In addition, as a deliverable for project Constellation, NAC stereo observations for a large area comprising the rim of Shackleton over to the peak near the rim of Spudis crater has been reduced into a large high-resolution DTM with 4m postings, which can be downloaded here:

There is limited potential to collect the additional observations required to enable the creation of additional polar DTMs in other locations near the geographic lunar south pole because of LRO orbital constraints. Please contact Dr. Noah Petro, the LRO Project Scientist, for additional informaiton regarding how to request additional LROC imagey of the south polar region.

4.2.2.3 LROC NAC DEM: Photoclinometry

The principle of photoclinometry, also called "Shape from Shading" or SfS, is that nadir images with different lighting conditions (solar incidence and azimuth) can enable mathematical solutions to determine the shape and topography of the illuminated surface. As described by Alexandrov and Beyer (2018), SfS can be used to establish Digital Terrain Models from NAC frames with consistently higher spatial resolution (~1-2 m/pixel) than that provided by the conventional SOCET-SET approaches described in Section 4.2.2.2. These are produced using NAC images and photoclinometry processing, with LOLA 5 m/pixel product as a basis. This product reverts to LOLA data for unilluminated areas in NAC images.

The quality of this product, which includes an SfS DTM, a maximally lit orthomosaic, and individual orthoimages of each import NAC image, is limited by the availability of NAC coverage and illumination conditions. A small number of SfS models have been created to support uncrewed NASA missions to the poles, but as of these writing these SfS models are not available for download or use. However, the creation of additional SfS models can be supported if sufficient NAC images with appropriate properties are available for the region of interest; please contact Dr. Noah Petro, the Artemis Spatial Data Lead, or Dr. Ross Beyer, the SfS model development lead, for additional information.

4.3 DERIVED PRODUCTS

Derived products are created by leveraging foundational products to interrogate or emphasize specific attributes of the surface. Software packages exist, such as Geospatial Data Abstraction Library (GDAL), that can programmatically generate the products from topographic data products. For example, see gdaldem for instructions on how to create the products discussed in this section. Products and methods that are already created for the lunar south pole are provided where available.

4.3.1 Slope Map

Slope maps are raster products that capture the angle between the observed surface and a horizontal reference plane. These can be derived from any topographic data product using a variety of algorithms at the desired spatial baseline. Slope maps can be used to identify surface hazards relevant to terrain use as well as characterize geological attributes.

Slope maps for the lunar south pole (latitudes > 87 deg. S) are currently available at 5 m/pixel, derived from the South Pole LOLA DEM Mosaic (described in Section 4.2.2.1) using Horn's Method, a standard averaging method to calculate slope from eight neighboring cells/pixels about a center cell/pixel where a third-order finite difference equation is used to produce an estimate of an average slope within an 8-cell neighborhood of a central cell.

PGDA - South Pole LOLA DEM Mosaic (nasa.gov)

Slope maps for individual sites of interest at 5 meters per pixel were derived using a different method. For these maps, slope was calculated as arccos(Nz) where Nz is the z-component of the unit normal surface vector. The latter is computed with Matlab's surfnorm routine, which takes a finite difference across the central pixel in the X and Y directions to define two vectors in the slope plane and then takes their cross product to get the surface normal to that plane. These local maps are available here:

PGDA - High-Resolution LOLA Topography for Lunar South Pole Sites (nasa.gov)

These slope products have stated median RMS errors of ~1.5-2.5 degrees. Slope derivation and error analyses are fully described in Barker et al (2021).

4.3.2 Shaded Relief Map (Hillshade)

Shaded Relief Maps, also known as Hillshade Maps, are raster images generated by modeling illumination from an artificial light source across a topographic data product. These depict surface relief using hypsographic tinting and surface contour density. In other words, hillshades emphasize changes in surface elevation using artificial light and shadows on terrain from a specified angle and altitude of the sun.

Hillshade maps can be generated from any available topographic data product using standard tools in GIS software, including commonly used software packages including the Geospatial Data Abstraction Layer (GDAL), ESRI's ArcGIS, and QGIS. Hillshade maps for the lunar south pole (latitudes poleward of 87 degrees) generated from the South Pole LOLA DEM Mosaic are available here:

PGDA - South Pole LOLA DEM Mosaic (nasa.gov)

This 5 m/pixel hillshade product was generated using the GDAL hillshade tool (gdaldem) with a solar incidence angle of 45 degrees from vertical and an azimuth angle of 45 degrees. Note: This is a physically unrealistic solar incidence angle for lunar polar regions but provides a good overview of local topographic relief.

For more information on illumination modeling, refer to Section 5.1.

4.3.3 Surface Roughness Analyses

Surface Roughness analyses encompass a broad array of surface characterization techniques relevant to describing the degree of variation in elevation across local scales. It is useful for understanding terrain hazards and traversability, as well as geological unit differentiation.

Surface Roughness can be estimated and reported through a variety of techniques and spatial scales. In general, surface roughness is either calculated directly from topographic data, or determined through either photometric assessments of imagery data or determined from radar data. Here, we summarize applications of various techniques.

4.3.3.1 Surface Roughness Products

Surface roughness can be estimated directly from topographic data products using a variety of techniques. The minimum spatial resolution and baseline for the roughness product is limited by the resolution of the topographic data. In general, estimates of surface roughness derived from topographic data are closely correlated with the slope determined for a terrain.

A commonly used metric to assess surface roughness is the Topographic Ruggedness Index (TRI), a measure of elevation variability between a central pixel and its neighboring eight pixels (typically using techniques similar to Horn's method). It calculates the difference in elevation values from a center cell and the eight cells immediately surrounding it. Then it squares each of the eight elevation difference values to make them all positive, sums them, and takes the square root. More information is available here:

Topographic Ruggedness Index (usna.edu)

4.3.3.2 Estimates from Imagery

Surface roughness can also be estimated from imagery and radar measurements, offering measurements at different spatial resolutions independent of topographically derived products. Roughness estimates can be determined in several ways:

Phase ratio observations. Planetary surfaces exhibit light backscattering and forward scattering properties based on particle size, distribution, and orientation. In other words, surface roughness affects the phase function of a material, meaning that surfaces with different roughness characteristics will scatter light differently. Ratios of images taken at different phase angles (co-registered images captured with different incident / emission angles) suppresses the signal from albedo variations, emphasizing differences in roughness and related physical properties. This technique is sensitive to roughness differences at the scale of the incoming light wavelength, which in principle can enabling characterization of roughness on spatial scales significantly smaller than the spatial resolution of imagery data (e.g., Kaydash et al., 2012).

Large incidence angle imagery: Imagery taken with large solar incidence angles (~55-80 degrees) includes significant shadowing and shading from topographic facets. Assuming similar albedo distributions, measurements of standard deviation in pixel values correlate with surface roughness, i.e., a rougher surface will include more shadows than a smoother surface and therefore be associated with a higher standard deviation in pixel brightness. This technique estimates surface roughness at spatial scales tied to imagery data. For instance, LROC WAC images can be used as a proxy for roughness at 500 m scales, while LROC NAC images can be used as a proxy or roughness at 2.5 m scales. This technique is useful where stereo pairs and/or phase ratio observations are unavailable.

Radar Measurements: Radar instruments measuring the lunar surface detect changes in signal polarization, which can be modified by interaction of the radar wave with the lunar surface during surface reflection and subsurface scattering. The Circular Polarization Ratio (CPR) provides a quantitative measure of changes in polarization, and is strongly correlated with surface roughness at various scales, most strongly at ~100 m (e.g., Jawin et al., 2014)

4.3.4 Aspect-Slope Map

Aspect-Slope maps simultaneously show the aspect (direction) and degree (steepness) of slope for a terrain. These can be derived from any topographic product using standardized functions such as the gdaldem routines that are built into the GDAL software.

5.0 MODELING ANALYSES AND ASSUMPTIONS

5.1 LOLA ILLUMINATION ANALYSIS

The LRO LOLA Instrument team has leveraged the LOLA dataset to to simulate average illumination conditions over the 18.6-year lunar precession cycle (Mazarico et al., 2011). Illumination models leverage local topography with the orbital positions of the Earth, Moon, and Sun to derive illumination conditions across the lunar surface at a specified time or time range. These models may also consider surfaces that are illuminated through “double-bounce” photons (*i.e.,* a surface may not experience direct illumination but may be secondarily illuminated by light reflected from local terrain). LOLA south polar models and additional background information are available here:

PGDA - Lunar Polar Illumination (nasa.gov)

These models are available at 240 m/pixel for latitudes > 65, 120 m/pixel for latitudes >75, and 60 m/pixel for latitudes >85. Currently, several types of illumination model are available at the above link:

- **Solar Illumination:** This product indicates the percentage of model timesteps where a pixel was sunlit by any fraction of the solar disc.
- **Earth Visibility:** This product indicates the percentage of model timesteps where a pixel was lit by any fraction of the Earth disc.
- **Sky Visibility:** This product indicates the solid angle of sky not obscured by topography visible from each pixel.
- **Permanent Shadow:** This product indicates areas receiving no sunlight over the 18.6-year lunar precession cycle.

Using similar techniques, higher-resolution products (5 m/pixel) can be requested for a specified time or time range and/or elevation above the surface (please contact Dr. Noah Petro, the SMD Artemis Spatial Data Lead, for additional information). For example, solar illumination at 5 m above the surface of the local and surrounding terrain may be a relevant product for planning solar power arrays. More nuanced models can also be produced accounting for scattered light, percentage of visible solar/Earth disc and/or accounting for time variability in Earthshine or solar flux.

The revised LOLA DEM products and processing methodology are described in Barker et al., (2021). More information about the derivation and properties of these models including detailed data descriptions are in the LBL files on the PDS are available at:

PGDA – South Pole LOLA DEM Mosaic

5.2 EARTH SHINE MAP

Earthshine is affected both by position relative to the local horizon and time-variable intensity. As defined in Glenar et al. (2018), in the context of lunar exploration, earthshine is the combined irradiance from reflected sunlight and thermal emission from Earth that illuminates the Moon.

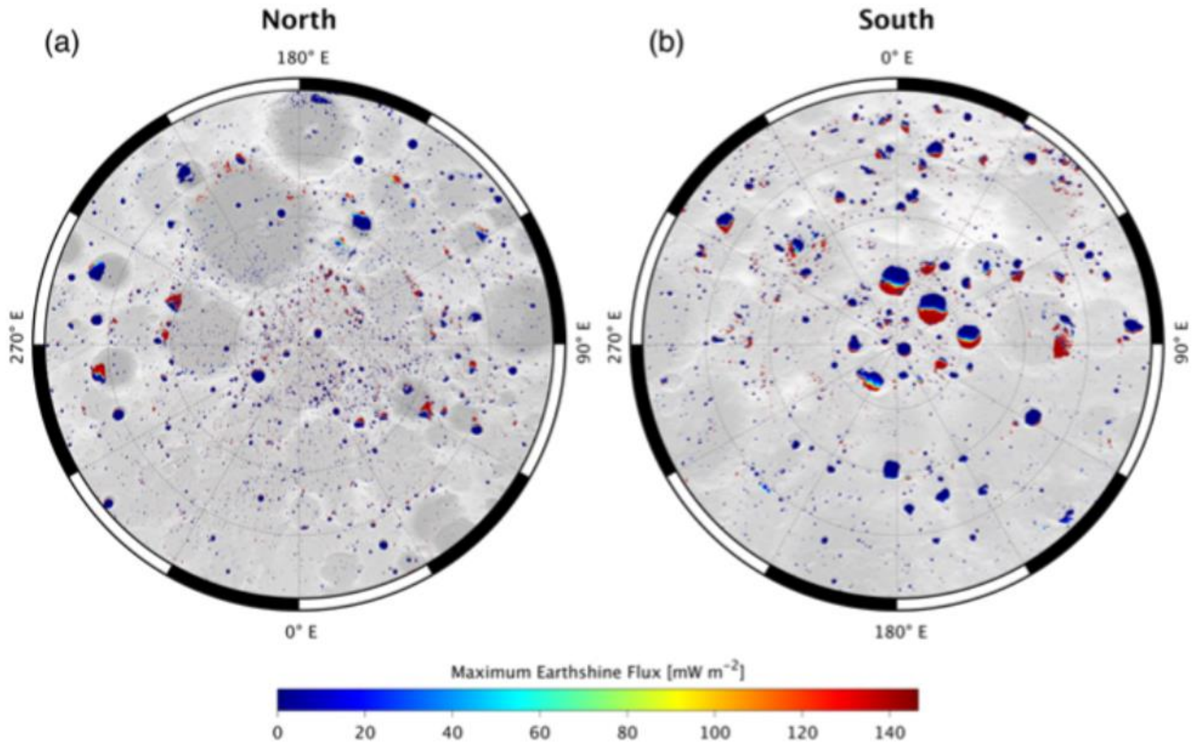

Figure 5.2.1 Maximum Earthshine flux incident on lunar PSRs at the north (a) and south (b) poles across one 18.6-year lunar processional cycle. Figure reproduced from Kloos and Moores (2019). The Earthshine flux is overlaid on topography (grayshade).

6.0 LUNAR TERRAIN CHARACTERISTICS

The following tables describe characteristics inherent to the lunar south pole region(Defined in the 2020 NASA Lunar Exploration Plan as the region within six degrees of latitude of the geographic lunar south pole) - and are provided as a reference for vehicle design in correlation with system requirements. Global slope distribution data, that is also applicable at the south pole is available in SLS-SPEC-159 Design Specifications for Natural Environments for design purposes per HEOMD-003.

The lunar south pole terrain incorporates the following discrete features, where (+ or -) means upslope/downslope.

Table 0-1 Slopes Inherent to Lunar South Pole Region

Max Slopes (°)	% South Pole Surface Area with these Slopes

0-5 (+ or -)	25%
5-10 (+ or -)	32%
10-15 (+ or -)	23%
15-20 (+ or -)	12%
20+ (+ or -)	8%

Note: Approximate areal extent of terrain with stated slopes (over a 5 m baseline) derived from the South Pole LOLA DEM Mosaic covering latitudes poleward of 87 deg. S. The derivation of this slope map is discussed in greater detail in section 4.3.1, and the DEM is described in section 4.2.2.1. The slope map was derived using Horn's method and is available at 5 m/pixel with a stated median RMS slope error ~ 1.5 - 2.5°. More information on source data, slope derivation, and error estimation is available in Barker et al (2021) and here:
PGDA - South Pole LOLA DEM Mosaic (nasa.gov)
PGDA - High-Resolution LOLA Topography for Lunar South Pole Sites (nasa.gov)

Table 0--2 Lunar Regolith Trafficability Parameters

Symbol	Description	Value
n	Exponent of sinkage	1
kc	Cohesive modulus	1400 N/m2
kϕ	Frictional modulus	830,000 N/m3
ϕ	Angle of internal friction	35 degrees
c	Cohesive strength of soil	170 N/m2
γ	Soil weight density	2470 N/m3
K	Coefficient of soil slip	0.018 m

Note: Figures derived from Lunar Sourcebook (1991), which in turn was based on in-situ measurements performed by the Apollo astronauts, and the reader is referred to chapter 9 of that work for detailed information on the geotechnical properties of the lunar surface. Lunar regolith characteristics may vary, including the potential for ice mixing with regolith in/near permanently shadowed regions (PSRs). For further clarification reference the Cross-Program Design Specification For Natural Environment (DSNE) SLS SPEC-159 Section 3.4 Lunar Surface Operational Phases.

7.0 EXAMPLE USE CASES LEVERAGING LUNAR SURFACE DATA

7.1 BASECAMP LOCATION CHARACTERISTICS (PLACEHOLDER)

7.2 MOBILITY USE CASES

The following mobility use cases correspond to the use cases defined in the Lunar Terrain Vehicle (LTV) Concept of Operations document LTV-CONOPS-001. Table 7.2-1 shows each use case may have different expected levels of performance across capabilities and represent notional categories of expected operations that mobility assets must conduct to complete the majority of the currently anticipated Artemis mission objectives. These examples do not represent definitive statements of operational mission priorities, nor do they encompass all possible exploration mobility activities on the surface of the Moon.

Table 0-1 Mobility Use Cases

Ex.	Capability/ Traverse Type	Driving	Availability	Expected Cargo	Expected Distance	Expected Duration (Traverse Time)	Frequency (per year)
1	**Scouting and Utilization**	Hybrid*	Continuously (uncrewed and crewed mission timeframes)	Science payloads and/or small cargo	Local (TBD range)	Varies	Frequent (many per month)
2	**Crew sortie**	Hybrid*	Crewed mission timeframes only	Science payloads, small cargo, plus crew, EVA tools	Within walk-back range	Short (~hours)	Infrequent (~daily) during crewed missions
3**	**Large Logistics**	Hybrid*	Crewed mission timeframes only	Stressing-Heavy cargo	Local (TBD range)	Short (~hours)	Infrequent, likely only during crewed missions
4**	**Long Uncrewed Science Traverse**	Uncrewed/ teleops	Continuously during uncrewed timeframes only	Science payloads	Long (TBD range)	Long (days or months)	Frequency TBD
5**	**Exploring PSRs**	Hybrid*	Continuously during uncrewed timeframes only	Science payloads, with or without crew/tools	Range TBD	Short (~hours)	Frequency TBD
6	**Cooperative Exploration (multiple mobility assets)**	Hybrid*	Crewed mission timeframes only	Science payloads, crew, tools, cargo/logistics	Extend past walk-back range	Potentially long cooperative traverses	Frequency (daily)

*Note: Hybrid suggests the traverse can be driven by both crewed operations and uncrewed operations (teleoperations).

**Note: Representative traverses for these use cases provided in Section 7.3.

7.3 REPRESENTATIVE TRAVERSES

The following examples represent notional, representative traverses that lunar mobility assets will need to be able to conduct and were chosen due to the variety of conditions and demands the vehicle may encounter. Examples below include relocation of logistics around the Artemis Base Camp (ABC), a long uncrewed science traverse, and a traverse into a permanently shadowed region (PSR). Note that these are example traverses only and do NOT represent definitive statements of operational mission priorities or profiles, and they do NOT encompass all possible exploration activities or destinations on the surface of the Moon. These examples are also not directly linked together unless explicitly stated. Therefore, details, acronyms, and labels in one example should not be associated to another example. Furthermore, all traverses described here are assumed to be carried out during illuminated portions of the lunar year and subsequent planning efforts will have to account for when actual missions are planned, and thus are likely to change. Integrated technical solutions to meet the variety of terrain encountered will need to be developed with limited data. Lunar mobility asset performance capability should meet the system requirements (threshold) with a stretch goal of increasing performance (objective). All of these traverses described herein are also described in HEOMD-410, “Lunar Reference Traverses”. The purpose of this text is to provide additional context and clarifying textual information provided in HEOMD-410, a data managed product. Vector data files of the traverses in HEOMD-410 are available upon request.

7.3.1 Large Logistics Transfer

The large logistics transfer representative traverse is outlined in Example 6 of the HEO-410 document. This example traverse involves a logistics transfer scenario where pre-deployed supplies are transferred along two points on the Connecting Ridge between Shackleton and de Gerlache craters using a mobility asset, over a 1.3 km traverse (Figure 7.3.1). Elevation and slope profiles are provided graphically in Figure 7.3.2. A table outlining slope statistics derived from an LROC Narrow Angle Camera Digital Elevation Model of this region is provided in Table 7.3-1. Relevant to LTV, this example traverse could include a maximum transport mass (cargo) over a shorter distance in the vicinity of Artemis Base Camp (known terrain), with lower speeds. Crew may be present to load/unload logistics, and the LTV may be driven by the crew during an EVA to relocate large logistics packages.

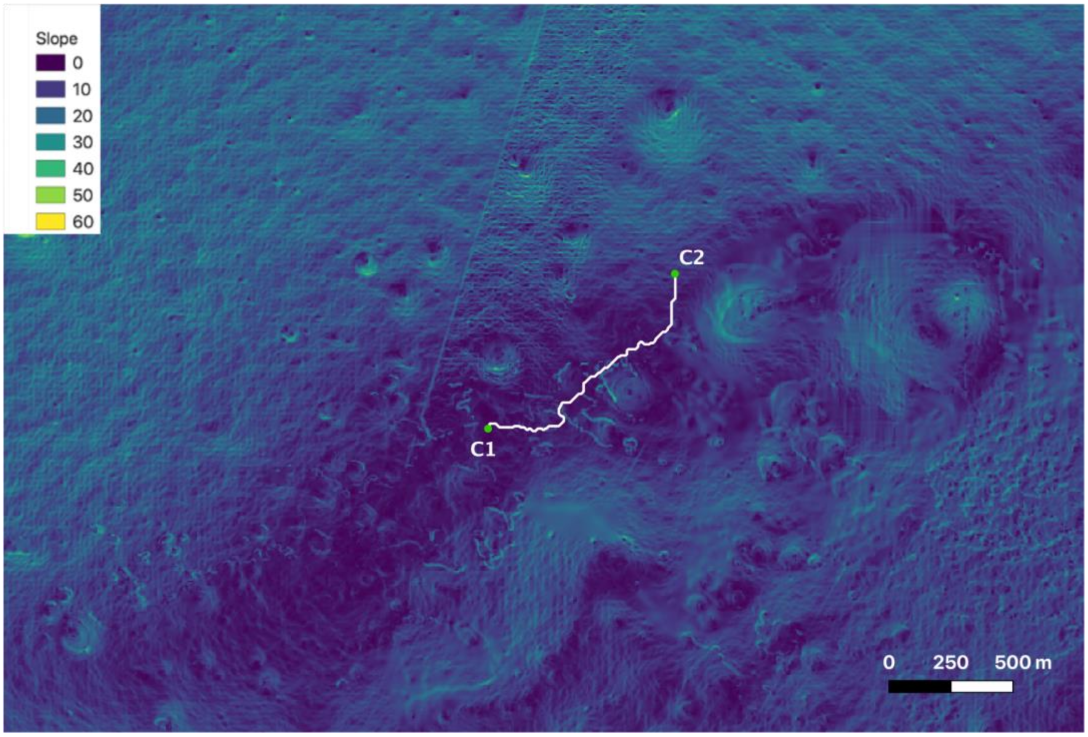

Figure 0.1 HEOMD-410 Example 6: Traverse between two points C1 (89.468° S, 222.6° E) and C2 (89.500° S, 222.1° E) on the Shackleton - de Gerlache connecting ridge. Basemap is slope information derived from USGS Astrogeology Science Center's Moon LRO South Pole DEM (https://astrogeology.usgs.gov/search/map/Moon/LRO/MOON_LRO_NAC_DEM_89S210E_4mp) using Horn (3x3) algorithm.

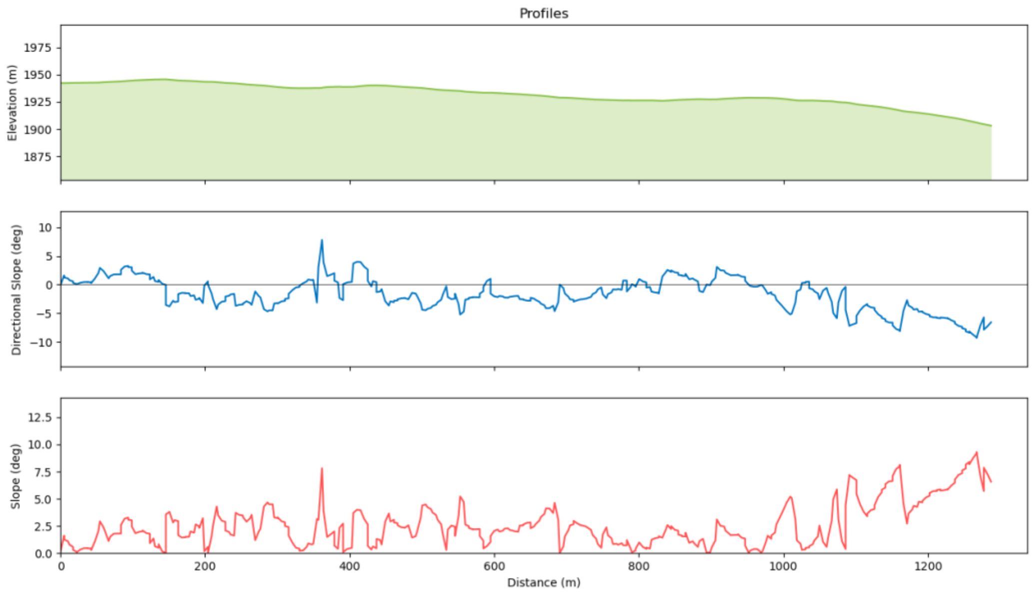

Figure 0.2 Elevation, Directional Slope, and Slope profiles for HEOMD-410 Example 6 derived from USGS Shackleton DTM.

Table 0-2

C1 to C2 Traverse Slope Statistics	
Minimum	0.17°
Maximum	9.76°
Mean	3.26°
Standard Deviation	1.88°

7.3.2 Long Uncrewed science traverse

HEO-410 Example 4 is an example of a prospective uncrewed traverse using the LTV. HEO-410 is based on the traverse developed in Speyerer et al. 2016 (Figure 7.3.3), as a representative example to provide options for LTV utilization that enable a variety of science and prospecting use cases and maximizes movement time between Connecting Ridge (CR), Shackleton Rim (SR), and Permanently Shadowed Region (PSR) points. As noted by Speyerer et al. 2016 (summarized here: http://lroc.sese.asu.edu/posts/937) this traverse does not include specific science station stops and does not assume a specific instrument suite on the vehicle; it is instead designed to maximize opportunities to achieve science and exploration opportunities subject to future instrument selection and operations plan development, while keeping the vehicle illuminated for most of a calendar year. In this scenario, the vehicle lands at the site designated CR1 and the LTV may rove between CR2 and CR3 to minimize nighttime duration. The total traverse distance is 38 km, and the maximum darkness duration would be 108 hours. Traverses to SR-1, SR-2, SR-3, and into PSR-1 from the CR-1 location are feasible during illuminated periods, examples of which are provided in Figures 7.3.3-7.3.5.

Relevant to LTV, this example traverse includes examples of representative traverses designed to avoid obviously hazardous routes, with smaller transport mass (science payloads, no crew/cargo), over relatively long distances and long durations.

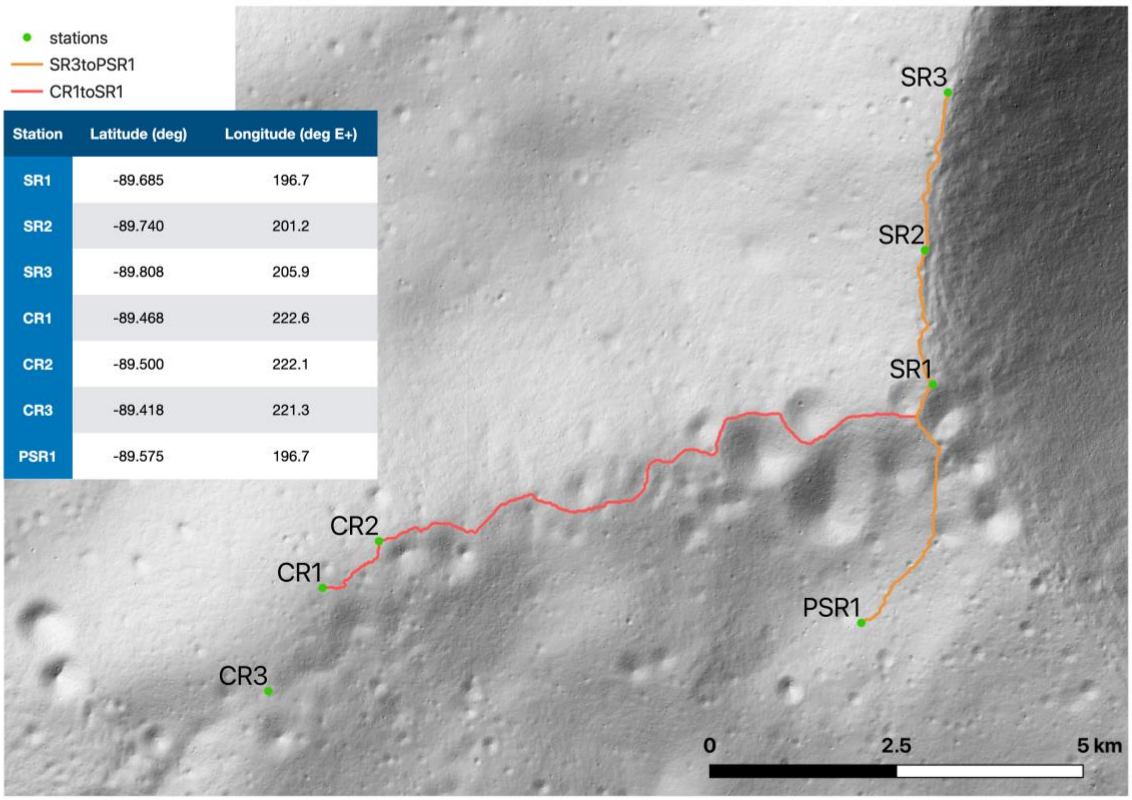

Station	Latitude (deg)	Longitude (deg E+)
SR1	-89.685	196.7
SR2	-89.740	201.2
SR3	-89.808	205.9
CR1	-89.468	222.6
CR2	-89.500	222.1
CR3	-89.418	221.3
PSR1	-89.575	196.7

Figure 0.3 Example of an uncrewed traverses focused on achieving science and exploration objectives and maximizing mobility in the absence of human crews, derived from Speyerer et al. 2016. Grayscale basemap is a synthetic hillshade image derived from the 5 m/pixel LOLA polar data product. Hillshade was generated with default parameters (solar azimuth: 315°; solar elevation: 45°) to quickly view terrain and thus not realistic illumination conditions.

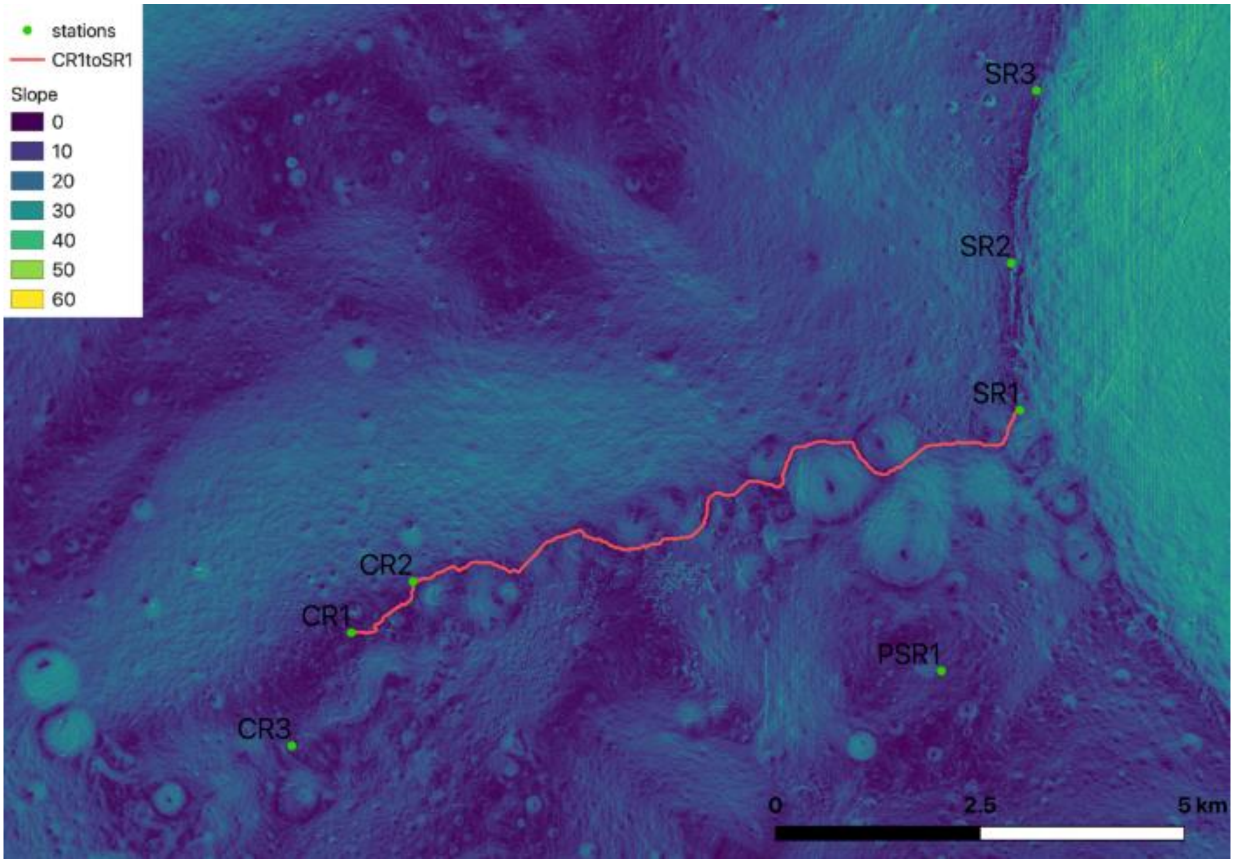

Figure 0.4 HEO-410 example 4 representative traverse from stations CR1 to SR1 on a slope map derived from a LROC Narrow Angle Camera Digital Elevation Model of the Shackleton - de Gerlache region.

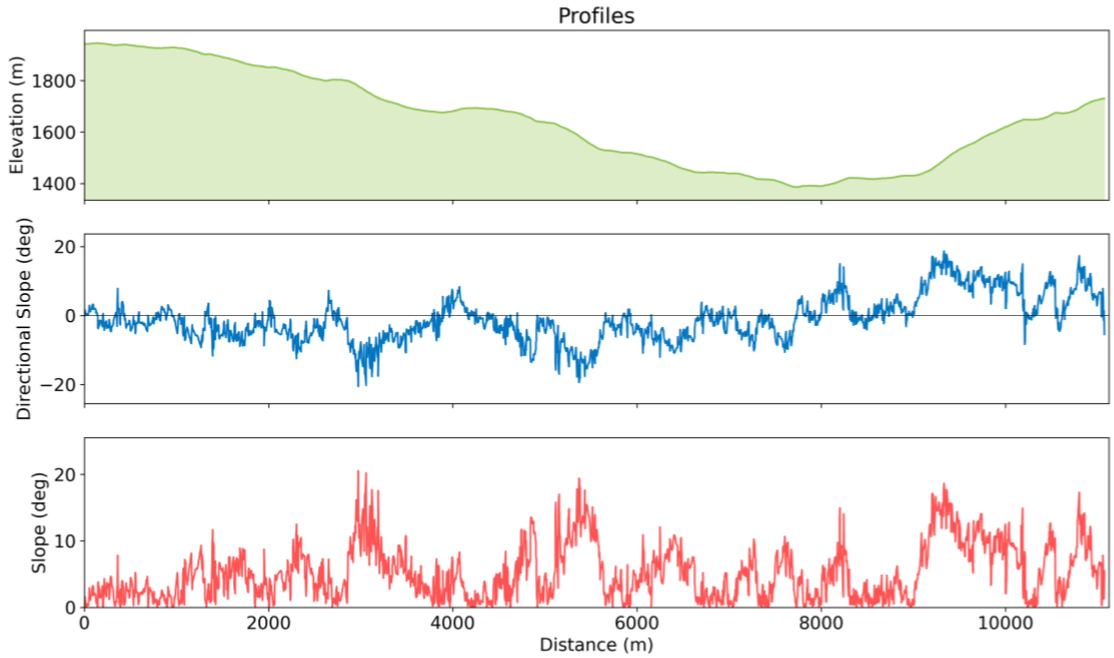

Figure 0.5 Elevation, Directional Slope, and Slope profiles for traverse path shown in Figure 7.3.4 from CR1 to SR1 extracted from a LROC Narrow Angle Camera Digital Elevation Model of the Shackleton - de Gerlache region

CR1 to SR1 Slope Stats	
Minimum	0°
Maximum	20.51°
Mean	5.17°
Standard Deviation	4.01°

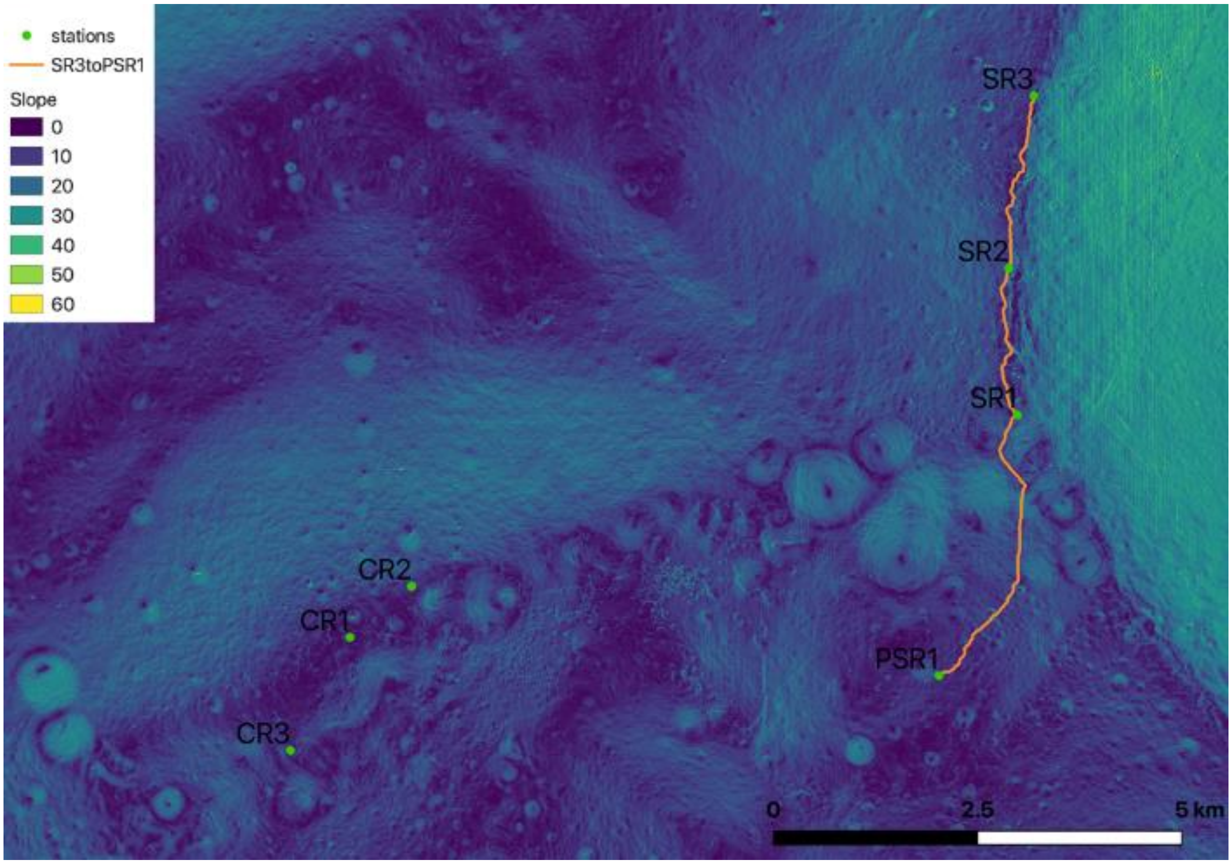

Figure 0.6 HEO-410 example 4 representative traverse from stations SR3 to PSR1 overlain on a slope map derived from a LROC Narrow Angle Camera Digital Elevation Model of the Shackleton - de Gerlache region.

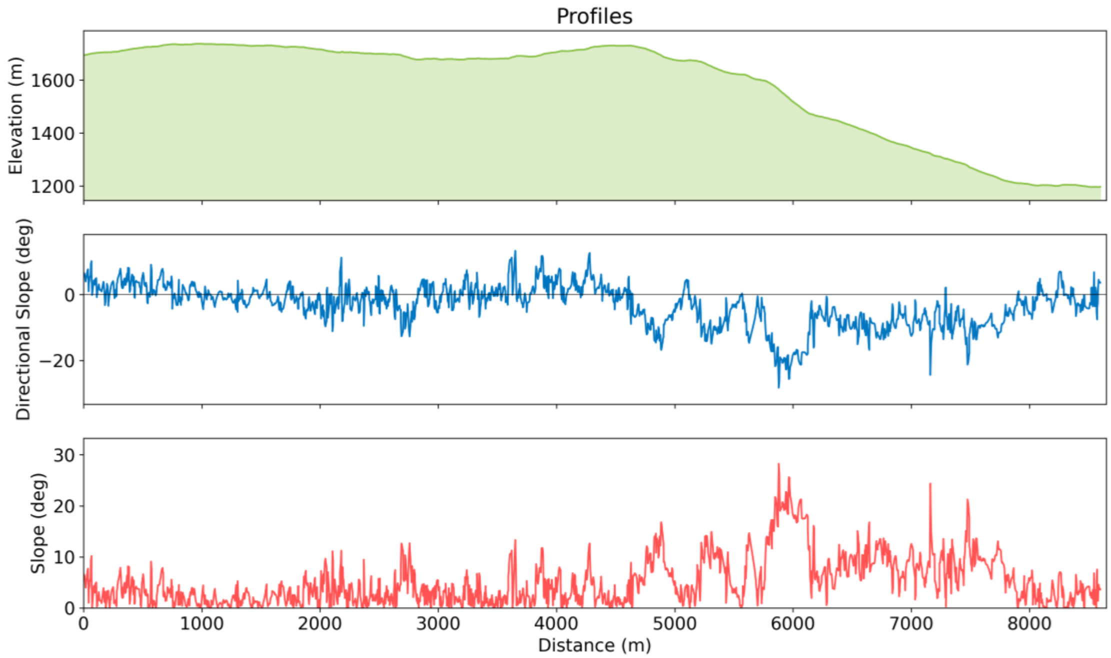

Figure 0.7 Elevation, Directional Slope, and Slope profiles for traverse path shown in Figure 7.3.6 from SR3 to PSR1 extracted from an LROC Narrow Angle Camera Digital Elevation Model of the Shackleton - de Gerlache region.

SR3 to PSR1 Slope Statistics	
Minimum	**0°**
Maximum	**28.26°**
Mean	**5.24°**
Standard Deviation	**4.69°**

7.3.3 Traverse into crater/PSR

This example is based on HEO-410 Example 5 and provides examples of prospective crewed traverses designed to enable the exploration of cold traps near the Shackleton - de Gerlache Connecting Ridge near Spudis crater. This scenario assumes a landing at the CR1 (89.468° S, 222.6° E) location described in Section 7.3, from HEO-410 Example 4. This scenario also assumes that the surface mission increment enables at least two rover-based traverses per mission. The PSR number labels are relevant to the figures in which they appear and are not universally recognized labels. Figure 7.3.9 shows representative elevation and slope profiles, which are summarized in Table 7.4.1. Figure 7.3.11 shows a representative round-trip traverse from CR1 to PSR3; Figure 7.3.12 shows the elevation and slope profiles, which are summarized in Table 7.4.2. Relevant to LTV, this example traverse includes challenging terrain (steep slope), with smaller transport mass (crew and science payloads, including deployed experiments and sample collection and acquisition hardware elements), over a shorter distance than that outlined in Section 7.3. Crew may or may not be present, and if uncrewed, the LTV may be tele-operated from a remote-control location.

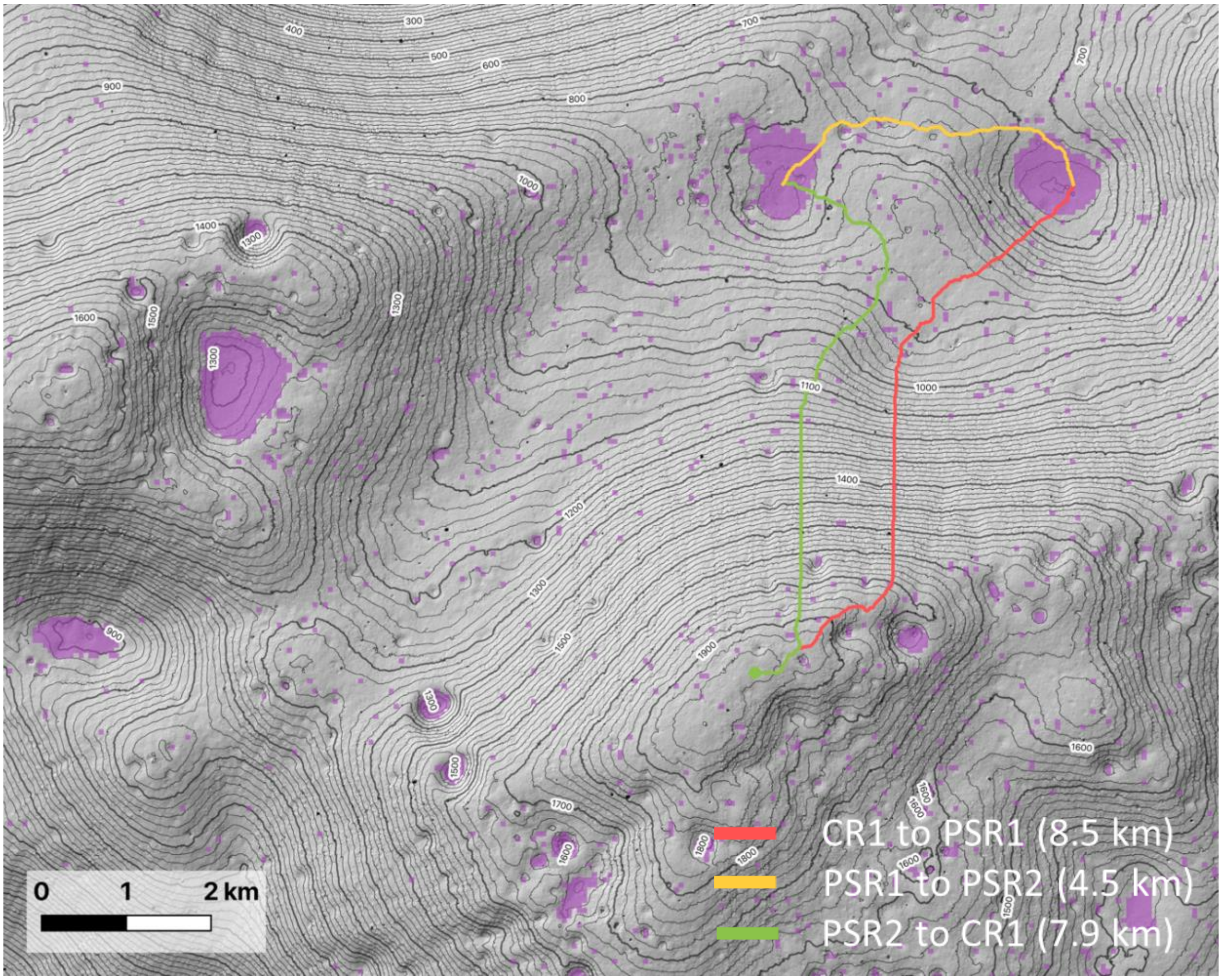

Figure 0.8 Topographic map of the Shackleton - de Gerlache Connecting Ridge, showing a round-trip traverse from CR1 to PSR1 and PSR2.

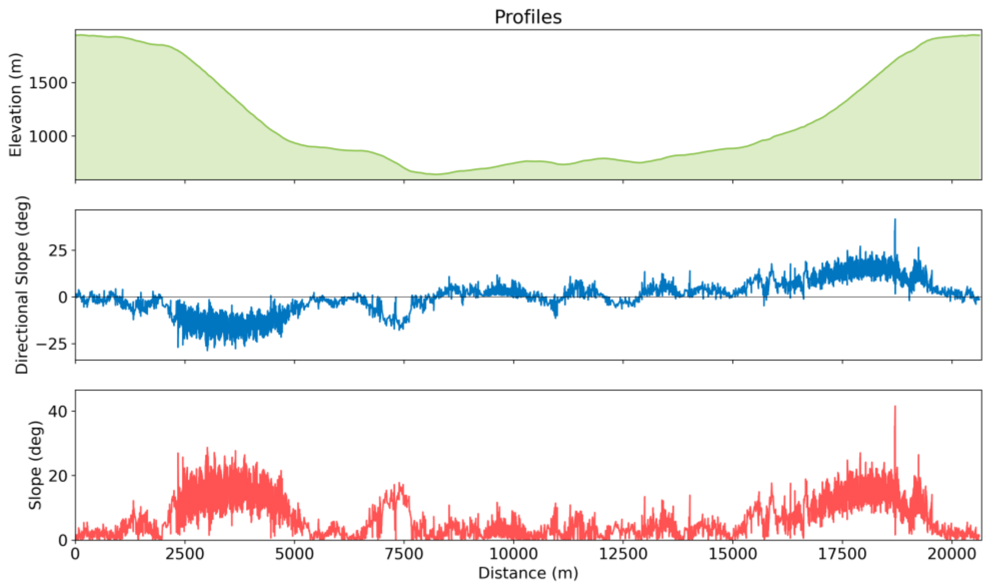

Figure 0.9 Elevation, Directional Slope, and Slope profiles for traverse path shown in Figure 7.3.9 from CR1 to PSR1 and PSR2 extracted from an LROC Narrow Angle Camera Digital Elevation Model of the Shackleton - de Gerlache region.

Table 0-3 Morphometry Summary of Traverse Outlined in Figure 7.3.10

Slope Stats	CR1 to PSR1	PSR1 to PSR2	PSR2 to CR1
Minimum	0.03°	0°	0°
Maximum	28.71°	11.66°	41.55°
Mean	8.4°	3.3°	7.8°
Standard Deviation	7.15°	2.03°	6.02°

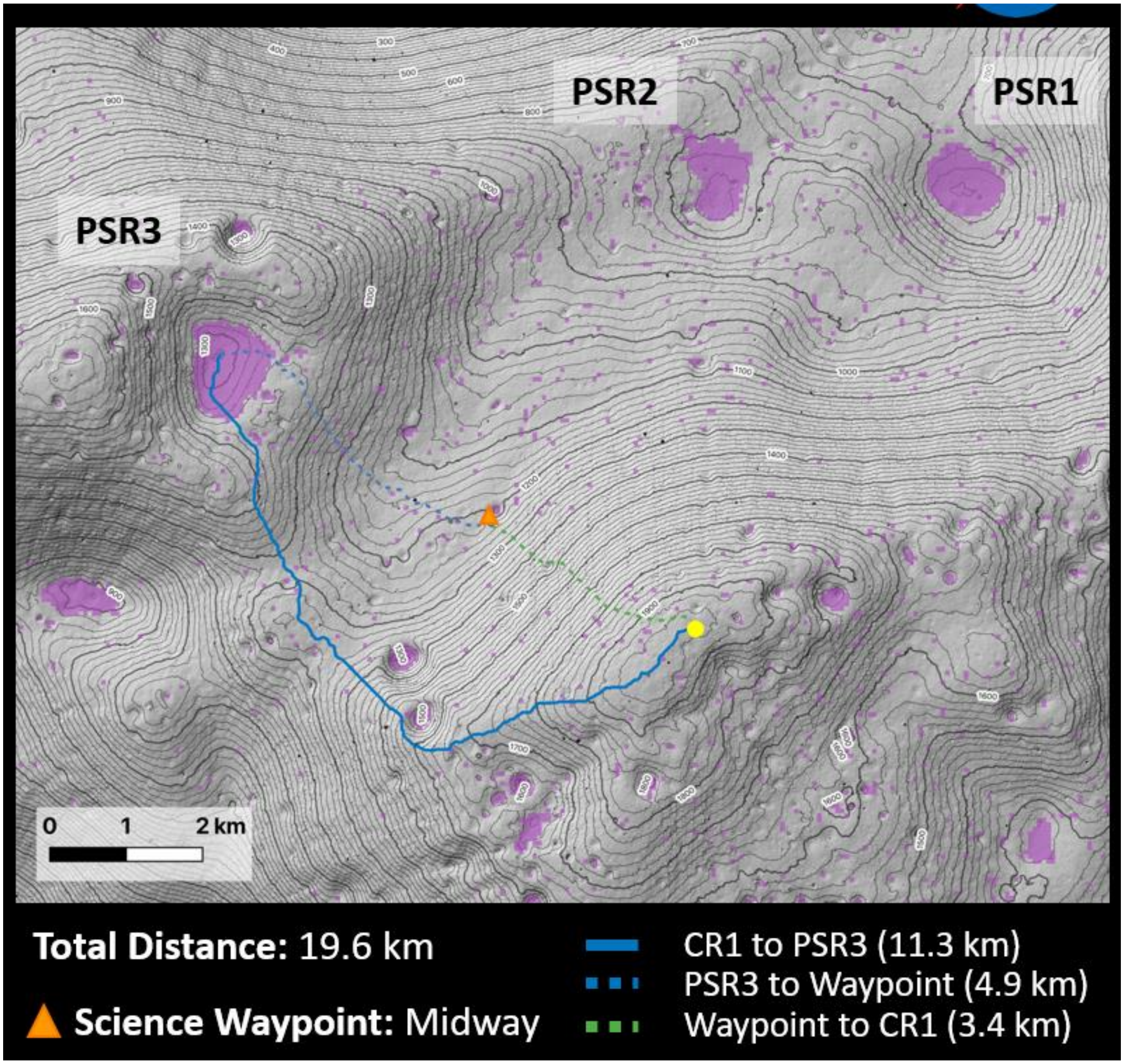

Figure 0.10 Topographic map of the Shackleton – de Gerlache Connecting Ridge showing a round-trip traverse from CR1 to PSR3.

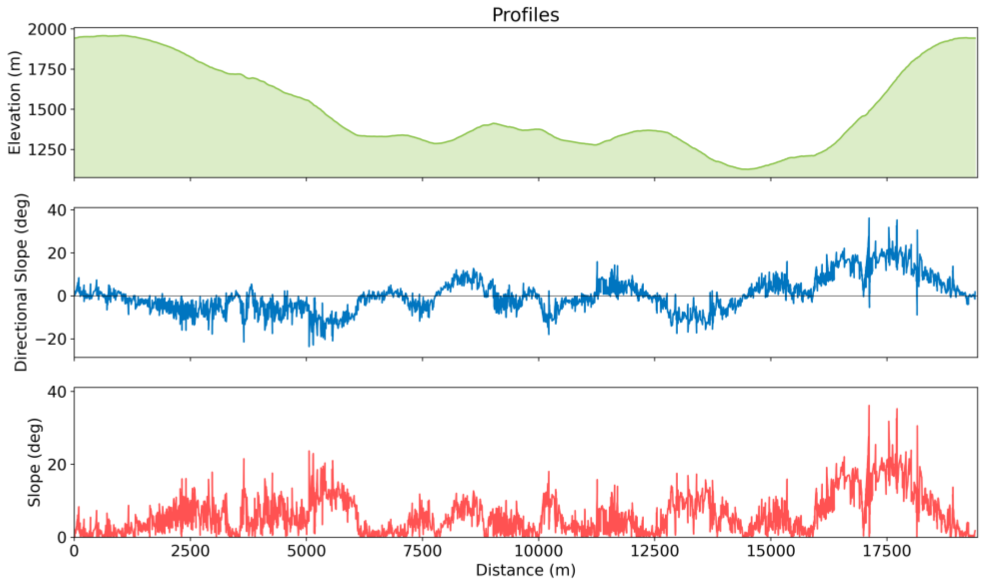

Figure 0.11 Elevation, Directional Slope, and Slope profiles for traverse path shown in Figure 7.3.11 from CR1 to PSR3 extracted from an LROC Narrow Angle Camera Digital Elevation Model of the Shackleton - de Gerlache region.

Table 0-4 Morphometry Summary of Traverse Outlined in 7.3.12

Slope Stats	CR1 to PSR3	PSR3 to Midway	Midway to CR1
Minimum	0°	0.02°	0°
Maximum	23.64°	17.5°	36.12°
Mean	5.28°	5°	11.65°
Standard Deviation	4.03°	3.74°	6.91°

APPENDIX A
ACRONYMS AND ABBREVIATIONS
AND GLOSSARY OF TERMS

A1.0 ACRONYMS AND ABBREVIATIONS

TABLE A1-1 ACRONYMNS

ACD	Artemis Campaign Development
CRaTER	Cosmic Ray Telescope for the Effects of Radiation
DEM	Digital Elevation Model
DLRE	Diviner Lunar Radiometer Experiment
DSM	Digital Surface Model
DTM	Digital Terrain Model
ESMD	Exploration Systems Mission Directorate
GDAL	Geospatial Data Abstraction Layer
LAMP	Lyman Alpha Mapping Project
LDEM	Lunar Digital Elevation Model
LEND	Lunar Exploration Neutron Detector
LEAG	Lunar Exploration Analysis Group
LOLA	Lunar Orbital Laser Altimeter
LRO	Lunar Reconnaissance Orbiter
LROC	Lunar Reconnaissance Orbiter Camera
MAPSIT	Mapping and Planetary Spatial Infrastructure Team
NAC	Narrow-Angle Camera
NSSDC	NASA's Space Science Data Coordinated Archive
PDS	Planetary Data System
PGDA	Planetary Geodesy Data Archive
SfS	Shape from Shading
WAV	Wide-Angle Camera

A2.0 GLOSSARY OF TERMS: LUNAR SURFACE TERMINOLOGY

The following terminology provides a common set of definition with respect to lunar terrain features that must be navigated and traversed by lunar mobility assets.

TABLE A2-1 LUNAR SURFACE TERMINOLOGY

3-Dimensional Distance	Measure of the cumulative distance along the elevation profile between two points to account for elevation gain and loss along a Euclidean or spherical distance

TABLE A2-1 LUNAR SURFACE TERMINOLOGY

Artemis Base Camp (ABC)	Site(s) chosen to serve as the core initial central point and hub for near-term and long-term lunar exploration. ABC is chosen for sustained lunar missions that will involve a series of robotic and crewed missions to ensure that the terrain, lighting, and nearby lunar resources meet the long-term surface operation objectives. ABC is made up of several zones (launch and landing zone, habitation zone, power productive and utility zone, resource zones, etc.) that will require some degree of maintenance, monitoring, support a direct operation without the presence of a crew on the surface
Coordinate Reference Frame	A solution that defines from observational data the specific numerical location of given points in the reference system
Crewed	Operations performed with local crew involvement
Datum	A reference point of set of reference points on the surface against which position measurements are made
Digital Elevation Model (DEM)	A digital representation of the bare ground topographic surface of a body that excludes a natural or built surface objects
Digital Terrain Model (DTM)	A digital representation of the bare ground topographic surface of a body that excludes natural or built surface objects but does include natural/built features as vector features
Digital Surface Model (DSM)	A digital representation of the bare ground topographic surface of a body and includes natural or built surface objects
Elevation	Vertical distance of a point or object above or below a reference surface or datum
Elevation Profile	Measure of elevation gain and loss along a line between two or more points
Equatorial Circumference of Moon	10916.4 km
Euclidean Distance	Measure of the straight-line distance from one point to another in the Euclidean space in cartesian coordinates. Also known as the Pythagorean distance
Figures of Merit (FOM)	Characteristics used to quantify the relative utility of a site (or other parameter), and form a basis of comparison between multiple factors
GIS	A Geospatial Information System (GIS) is a digital system designed to capture, store, manipulate, analyze, manage, and present spatial data
Gradient	The magnitude of a slope in the steepest direction. Defined as Change in Z / Change in X. A slope relative to the LTV is described by a max slope gradient and a gradient relative to the LTV planed direction of motion or angle of attack (LTV relative slope gradient)
Hazard	Physical feature that generates a risk for the LTV and prevents its progress. *Note: Hazardous obstacles are not defined here because LTV design (traverse threshold, traverse threshold angle, etc.) will dictate which obstacles are safe or hazardous
Height	Vertical distance above the local surface
Horn Method	An averaging method to calculate slope from eight neighboring cells/pixels about a center cell/pixel where a third-order finite difference equation is used to produce an estimate of an average slope within an 8-cell neighborhood of a central cell

TABLE A2-1 LUNAR SURFACE TERMINOLOGY

Landing Ellipse	The dispersed area (either 3 sigma or 99%-tile) on the lunar surface where the is vehicle is estimated to land with the landing site at the center of the ellipse
Landing Site	A vector point data type use to indicate the exact surface location of the landing site
Lunar Digital Elevation Model (LDEM)	Topographic dataset providing an elevation (km) above fixed lunar radius of 1737.4 km
Map Points	Vector data type used to symbolize coordinates of a single object or location at the surface
Negative Obstacle	Defined by a diameter (Ø) and a negative slope. On the lunar surface they are mostly craters.
Obstacle	Physical feature that can hinder LTV progress on the lunar surface (e.g., rock, crater, slope)
Offet	Shift in datasets relative to each other due to differences in processing or data preparation
Parking Lot	Larger area that can accommodate multiple landing ellipses
Pixel	The smallest addressable element in a raster image
Positive Obstacle	Defined by a step height and a positive slope. On the lunar surface they are mostly rocks. The positive obstacle step height is the distance between the surface and the maximum height of an obstacle
Radius of Moon	1737.4 km
Raster Image	A two-dimensional image as a rectangular matrix or grid of square cells, also known as pixels
Region	A geographic territory that encompasses a range of features, bound together by shared characteristics, either natural or connected to the territory explored during a mission
Region of Interest	Portions of a region of expected potential scientific or other exploration value
Regolith	The surficial layer of fragmented material (rocks, soil, and dust) that covers virtually the entire surface of the Moon
Selapoid	A smooth but irregular surface whose shape results from the uneven distribution of mass within and on the surface of the moon
Site	Location on the surface where a specific action takes place (e.g., landing, sampling, instrument deployment)
Site Plan	Similar to a terrestrial site plan, the lunar site plan is a developmental plan showing the growth of the Artemis Base Camp over time, that shows the locations, connections, and orientations of the ABC assets
Slope	Change in elevation across a certain distance (X meters)
Slope Map	A non-directional slope (degrees) at each map pixel location
Spatial Resolution	Spatial resolution is a measure of the smallest object that can be definitively resolved by the sensor, or the ground area imaged for the instantaneous field of view (FOV) of the sensor, or the linear dimension on the ground represented by each pixel
Spherical Distance	Measure of the line that connects two points along the surface of a sphere. Also known as orthodromic distance

TABLE A2-1 LUNAR SURFACE TERMINOLOGY

Terrain	Physical features of the lunar surface
Terrain Relative Navigation (TRN)	An autonomous, optical, or laser-based system for landmark recognition, spacecraft position estimation, and spacecraft retargeting
Terrain Surface Roughness	Quantified by the deviations in the direction of the normal vector of a real surface from its ideal form. The roughness is measured on a certain surface area
Traverse	Movement across the surface, either by crew or robotic assets that has a starting point and destination points and a path that connects two points
Uncrewed	Operations performed without local crew involvement
Vector	A data model that uses vertices with geographic locations to create geographic features such as points, lines, and polygons. Vector data asl may have associated spatial and non-spatial attribute data
Vehicle Footprint	The surface area bounded by the perimeter of the vehicle, with landing legs extended, on the lunar surface
Vehicle Plume Ejecta	Material that has been moved across the surface because of engine firing during descent/ascent
Zone	An area where regulations or requirements are uniform

APPENDIX B
REFERENCE MATERIAL

TABLE B1-1 REFERENCE SOURCES

Alexandrov, O., & Beyer, R. A. (2018). Multiview Shape-From-Shading for Planetary Images. Earth and Space Science, 5(10), 652–666. https://doi.org/10.1029/2018EA000390

Anderson, J. A., Sides, S. C., Soltesz, D. L., Sucharski, T. L., & Becker, K. J. (2004). Modernization of the Integrated Software for Imagers and Spectrometers. Abstract no. 2039. https://ui.adsabs.harvard.edu/abs/2004LPI....35.2039A

Barker, M. K., Mazarico, E., Neumann, G. A., Smith, D. E., Zuber, M. T., & Head, J. W. (2021). Improved LOLA elevation maps for south pole landing sites: Error estimates and their impact on illumination conditions. Planetary and Space Science, 203, 105119. https://doi.org/10.1016/j.pss.2020.105119

Gladstone, G. R., Stern, S. A., Retherford, K. D., Black, R. K., Slater, D. C., Davis, M. W., Versteeg, M. H., Persson, K. B., Parker, J. W., Kaufmann, D. E., Egan, A. F., Greathouse, T. K., Feldman, P. D., Hurley, D., Pryor, W. R., & Hendrix, A. R. (2010). LAMP: The Lyman Alpha Mapping Project on NASA's Lunar Reconnaissance Orbiter Mission. Space Science Reviews, 150(1), 161–181. https://doi.org/10.1007/s11214-009-9578-6

Heiken, G. H., Vaniman, D. T., & French, B. M. (1991). Lunar Sourcebook, A User's Guide to the Moon.

Henriksen, M. R., Manheim, M. R., Speyerer, E. J., Robinson, M. S., & Team, L. (2016). Extracting accurate and precise topography from LROC narrow angle camera stereo observations. The International Archives of Photogrammetry, Remote Sensing and Spatial Information Sciences, 41, 397.

Keller, J. W., Petro, N. E., & Vondrak, R. R. (2016). The Lunar Reconnaissance Orbiter Mission – Six years of science and exploration at the Moon. Icarus, 273, 2–24. https://doi.org/10.1016/j.icarus.2015.11.024

Keszthelyi, L., Becker, T. L., Sides, S., Barrett, J., Cook, D., Lambright, S., Lee, E., Milazzo, M., Oyama, K., Richie, J., Saleh, R., Shinaman, J., Sucharscki, T., Titus, T., Walldren, J., & Weller, L. (2013). Support and Future Vision for the Integrated Software for Imagers and Spectrometers (ISIS). Abstract no. 2546.

Kloos, J. L., & Moores, J. E. (2019). Mapping the Limited Extent of Earthshine within Lunar PSRs. Research Notes of the AAS, 3(9), 127. https://doi.org/10.3847/2515-5172/ab4195

Laura, J. R., & Beyer, R. A. (2021). Knowledge Inventory of Foundational Data Products in Planetary Science. The Planetary Science Journal, 2(1), 18. https://doi.org/10.3847/PSJ/abcb94

Martin, A. C., Grey, P. E., Henriksen, M. R., & Robinson, M. S. (2019). LROC NAC Feature Mosaics: An Effective Tool for Lunar Investigations. 2151, 7077. https://ui.adsabs.harvard.edu/abs/2019LPICo2151.7077M

Raney, R. K., Spudis, P. D., Bussey, B., Crusan, J., Jensen, J. R., Marinelli, W., McKerracher, P., Neish, C., Palsetia, M., Schulze, R., Sequeira, H. B., & Winters, H. (2011). The Lunar Mini-RF Radars: Hybrid Polarimetric Architecture and Initial Results. Proceedings of the IEEE, 99(5), 808–823. https://doi.org/10.1109/JPROC.2010.2084970

Robinson, M. S., Brylow, S. M., Tschimmel, M., Humm, D., Lawrence, S. J., Thomas, P. C., Denevi, B. W., Bowman-Cisneros, E., Zerr, J., Ravine, M. A., Caplinger, M. A., Ghaemi, F. T., Schaffner, J. A., Malin, M. C., Mahanti, P., Bartels, A., Anderson, J., Tran, T. N., Eliason, E. M., … Hiesinger, H. (2010). Lunar Reconnaissance Orbiter Camera (LROC) Instrument Overview. Space Science Reviews, 150(1), 81–124. https://doi.org/10.1007/s11214-010-9634-2

Smith, D. E., Zuber, M. T., Neumann, G. A., Lemoine, F. G., Mazarico, E., Torrence, M. H., McGarry, J. F., Rowlands, D. D., Head III, J. W., Duxbury, T. H., Aharonson, O., Lucey, P. G., Robinson, M. S., Barnouin, O. S., Cavanaugh, J. F., Sun, X., Liiva, P., Mao, D., Smith, J. C., & Bartels, A. E. (2010). Initial observations from the Lunar Orbiter Laser Altimeter (LOLA). Geophysical Research Letters, 37(18). https://doi.org/10.1029/2010GL043751

Spence, H. E., Case, A. W., Golightly, M. J., Heine, T., Larsen, B. A., Blake, J. B., Caranza, P., Crain, W. R., George, J., Lalic, M., Lin, A., Looper, M. D., Mazur, J. E., Salvaggio, D., Kasper, J. C., Stubbs, T. J., Doucette, M., Ford, P., Foster, R., … Charara, Y. (2010). CRaTER: The Cosmic Ray Telescope for the Effects of Radiation Experiment on the Lunar Reconnaissance Orbiter Mission. Space Science Reviews, 150(1), 243–284. https://doi.org/10.1007/s11214-009-9584-8

Speyerer, E. J., Lawrence, S. J., Stopar, J. D., Gläser, P., Robinson, M. S., & Jolliff, B. L. (2016). Optimized traverse planning for future polar prospectors based on lunar topography. Icarus, 273, 337–345. https://doi.org/10.1016/j.icarus.2016.03.011

Stickle, A., & Stoper, J. (2021). Final Report of the Lunar Critical Data Products Specific Action Team. Lunar Exploration Analysis Group (LEAG).

Vondrak, R., Keller, J., Chin, G., & Garvin, J. (2010). Lunar Reconnaissance Orbiter (LRO): Observations for Lunar Exploration and Science. Space Science Reviews, 150(1), 7–22. https://doi.org/10.1007/s11214-010-9631-5

Williams, J.-P., Greenhagen, B. T., Paige, D. A., Schorghofer, N., Sefton-Nash, E., Hayne, P. O., Lucey, P. G., Siegler, M. A., & Aye, K. M. (2019). Seasonal Polar Temperatures on the Moon. Journal of Geophysical Research: Planets, 124(10), 2505–2521. https://doi.org/10.1029/2019JE006028

APPENDIX C OPEN WORK

C1.0 TO BE SPECIFIED

The table To Be Specified Items lists the specific To Be Specified (TBS) items in the document that are not yet known. The TBS is inserted as a placeholder wherever the required data is needed and is formatted in bold type within carets. The TBS item is numbered based on the document number (i.e., **<TBS-xxxx-00x-00x>** is the first undetermined item assigned in the document). As each TBS is resolved, the updated text is inserted in each place that the TBS appears in the document and the item is removed from this table. As new TBS items are assigned, they will be added to this list in accordance with the above-described numbering scheme. Original TBSs will not be renumbered

TABLE C1-1 TO BE SPECIFIED ITEMS

TBD	Section	Description
TBS-xxxx-00x-001		

C2.0 FORWARD WORK

The table Forward Work lists the specific Forward Work (FWD) issues in the document that are not yet known. The FWD is inserted as a placeholder wherever the required data is needed and is formatted in bold type within carets. The FWD issue is numbered based on the document number (i.e., **<FWD-xxxx-00x-00x>** is the first forward work assigned in the document). As each FWD is resolved, the updated text is inserted in each place that the FWD appears in the document and the issue is removed from this table. As new FWD issues are assigned, they will be added to this list in accordance with the above-described numbering scheme. Original FWDs will not be renumbered.

TABLE C2-1 FORWARD WORK ITEMS

TBR	Section	Description
FWD-xxxx-00x-001		